Journal of Medicinal Chemistry

Article

Cite This: J. Med. Chem. 2018, 61, 2924−2936

pubs.acs.org/jmc

Antibacterial Activity Affected by the Conformational Flexibility in Glycine−Lysine Based α-Helical Antimicrobial Peptides

Tomislav Rončević,[†] Damir Vukičević,[‡] Nada Ilić,[†] Lucija Krce,[†] Goran Gajski,[§] Marija Tonkić,[∥,⊥] Ivana Goić-Barišić,[∥,⊥] Larisa Zoranić,[†] Yogesh Sonavane,[†] Monica Benincasa,[#] Davor Juretić,[†,▽] Ana Maravić,[*,○] and Alessandro Tossi[#]

[†]Department of Physics, Faculty of Science, University of Split, 21000 Split, Croatia

[‡]Department of Mathematics, Faculty of Science, University of Split, 21000 Split, Croatia

[§]Mutagenesis Unit, Institute for Medical Research and Occupational Health, 10000 Zagreb, Croatia

[∥]Department of Clinical Microbiology, University Hospital of Split, 21000 Split, Croatia

[⊥]School of Medicine, University of Split, 21000 Split, Croatia

[#]Department of Life Sciences, University of Trieste, 34127 Trieste, Italy

[▽]Mediterranean Institute for Life Sciences, 21000 Split, Croatia

[○]Department of Biology, Faculty of Science, University of Split, Ruđera Boškovića 33, 21000 Split, Croatia

Supporting Information

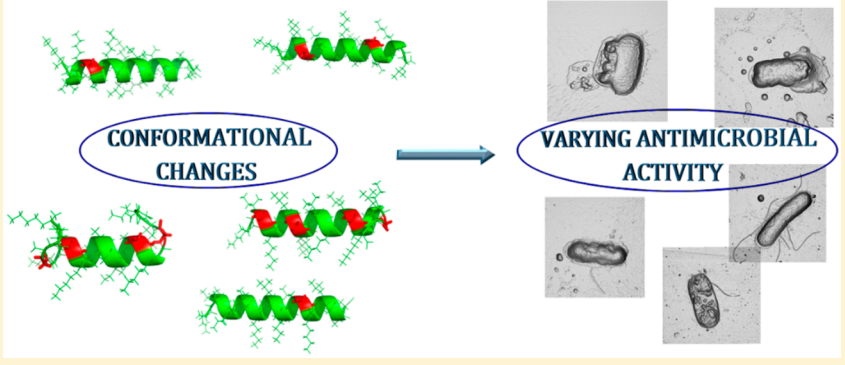

ABSTRACT: Antimicrobial peptides often show broad-spectrum activity due to a mechanism based on bacterial membrane disruption, which also reduces development of permanent resistance, a desirable characteristic in view of the escalating multidrug resistance problem. Host cell toxicity however requires design of artificial variants of natural AMPs to increase selectivity and reduce side effects. Kiadins were designed using rules obtained from natural peptides active against *E. coli* and a validated computational algorithm based on a training set of such peptides, followed by rational conformational alterations. In vitro activity, tested against ESKAPE strains (ATCC and clinical isolates), revealed a varied activity spectrum and cytotoxicity that only in part correlated with conformational flexibility. Peptides with a higher proportion of Gly were generally less potent and caused less bacterial membrane alteration, as observed by flow cytometry and AFM, which correlate to structural characteristics as observed by circular dichroism spectroscopy and predicted by molecular dynamics calculations.

INTRODUCTION

Over the past decades the rapid spread of antimicrobial resistance has become one of the most serious global health threats, as strains of human pathogenic bacteria capable of causing life-threatening infections have become resistant to most or all currently available classes of antibiotics.[1] Given the scarcity of new, effective drugs in the pipeline, colistin has become a last-resort antibiotic used for treatment of multidrug-resistant pathogens, but its effectiveness has been seriously compromised by the plasmid-mediated dissemination of the *mcr-1* gene.[2] For this reasons, the World Health Organization (WHO) designated carbapenem-resistant *Acinetobacter baumannii, Pseudomonas aeruginosa*, and *Enterobacteriaceae* (including the third generation cephalosporin-resistant ones) as "critical" to treat and a top priority target for which new antibiotics are urgently needed.[1]

Antimicrobial peptides (AMPs), endogenous effectors of the innate immune system of multicellular organisms, often show a broad spectrum activity against Gram-positive and Gram-negative pathogens, including multidrug resistant strains, and so are considered plausible candidates for development of new antibiotics.[3,4] Their mode of action frequently involves a

Received: December 13, 2017
Published: March 19, 2018

DOI: 10.1021/acs.jmedchem.7b01831
J. Med. Chem. 2018, 61, 2924−2936

Table 1. Sequence and Physicochemical Characteristics of Kiadins

peptide	sequence[a]	charge	H^c	μH^{rel} [d]	SI^{calc} [e]
PGLa-H[f]	KIAKVALKAL-NH_2	+4	−0.1	0.60	93
kiadin-1[f]	KIAKVALKALKIAK**G**ALKAL-NH_2	+7	−0.4	0.51	94
kiadin-2	KIAK**G**ALKALKIAKVALKAL-NH_2	+7	−0.4	0.45	92
kiadin-3	KIAK**G**ALKALKIAK**G**ALKAL-NH_2	+7	−0.7	0.50	94
kiadin-4	KI**G**KAL**G**KALKAL**G**KAL**G**KA-NH_2	+7	−1.4	0.73	91
kiadin-5	KIA**G**KA**G**KIAKIA**G**KA**G**KIA-NH_2	+7	−2	0.36	95
kiadin-6	KIALKALKALKAL**G**KALKAL-NH_2	+7	−0.1	0.55	93
melittin	GIGAVKLVLTTGLPALISWIKRKRQQ-NH_2	+6	0	0.30	17
colistin[b]	fatty acid-UTUU*U*L*L*UUT	+5			

[a]Residues conserved in >50% of peptide sequences are shaded gray. Gly residues likely affecting flexibility are in red. [b]U = diaminobutyric acid; the peptide has a cyclic backbone linking T the α-carboxyl to the γ-amino group of the 4th Dab residue. *L* = D-Leu. [c]Calculated using the CCS consensus hydrophobicity scale.[19] [d]Hydrophobic moment relative to a perfectly amphipathic helical peptide of 18 residues. [e]Predicted selectivity index by using the tool http://split4.pmfst.hr/mutator/ on a 1−95 scale. [f]Reference 9.

selective interaction with and subsequent disruption of bacterial membranes, leading to the formation of pores or other lesions in a manner that makes it difficult for bacteria to develop long-term resistance.[5] However, a potent cytolytic activity against bacteria is frequently accompanied by significant toxicity toward host cells, as shown for example by the bee venom peptide melittin.[6] It is not easy to find or design peptides that can effectively inactivate bacteria at concentrations sufficiently lower to those that damage host cells to avoid unacceptable side effects.

Some approaches involve abandoning the peptide backbone altogether and incorporating specific features of AMPs (e.g., the presence of cationic residues) onto polymer matrices (polysaccharides or polymethacrylates), exploiting the capacity for electrostatic and H-bonding interactions with membrane phospholipids either to obtain a direct antibacterial activity or to deliver covalently bound antibiotic cargo directed against both Gram-positive and Gram-negative bacterial strains.[7,8] These constructs have the advantage of gaining in selectivity and also proteolytic stability, but are complex to prepare and not amenable to biosynthesis.

Alternatively, approaches can be used to design more selective, canonical AMP sequences. This involves either subtly modifying natural AMP sequences to reduce toxicity while not affecting potency[9] or designing sequences de novo to have favorable characteristics, but it is not facile. It requires developing molecular descriptors that link biophysical properties to biological activity, in particular antimicrobial potency and high selectivity (QSAR methods).[10,11] Host defense peptides (HDPs), as ubiquitous natural AMPs vetted by evolution, are a good starting point for obtaining these descriptors, and anuran species, in particular, are an abundant and well explored source of HDPs.[12] By applying QSAR methods to sets of anuran peptides with known antimicrobial potencies and toxicities (in terms of minimal inhibitory concentration (MIC) toward *Escherichia coli* and HC_{50} values from hemolysis), we have previously designed adepantins, short linear peptides rich in Gly and Lys residues and with particularly high selectivity indices ($SI = HC_{50}/MIC$).[13] We here report a new class of Gly/Lys-rich peptides, named kiadins, obtained from either a template provided by the small natural HDP PGLa-H, as described previously,[9] or ab initio by using a comprehensive set of QSAR criteria.

Five kiadin peptides were selected for synthesis and in vitro activity testing against emerging Gram-positive and Gram-negative bacterial pathogens, including the carbapenem-resistant *Acinetobacter baumannii* and *Pseudomonas aeruginosa*, as well as the third generation cephalosporin-resistant *E. coli* and *Klebsiella pneumoniae*, while cyto/genotoxicity tests were conducted on human circulating blood cells. These peptides showed a variable activity, ranging from potent and selective to potent but toxic to almost inactive. Furthermore, it was possible to correlate potency to the effect of peptides on the bacterial membrane, as visualized by atomic force microscopy (AFM). Insight into how difference in sequence affected structuring as well as membrane interaction and insertion was also based on the correlation of experimental results with molecular dynamics simulations of the peptides in solutions and in the presence of a lipid bilayer. These findings are consistent with previous reports that activity depends on the positioning in the sequence of Gly residues and in general may benefit from an optimal flexibility index,[14−16] but this is modulated by amphipathicity requirements.

RESULTS AND DISCUSSION

Peptide Design. Kiadin-2 and -3 were designed by modifying a parent peptide, kiadin-1, itself derived from a natural AMP (PGLa-H)[9] (see Table 1). Kiadin-4 to kiadin-6 were ab initio designed by following a defined set of rules based on observed features from a set of natural peptides (see Supporting Information). Irrespective of the design procedure, the peptide sequences are sufficiently similar (≥50% conserved sequences) for us to consider them as a single kiadin family.

For the ab initio design procedure, applying design rules too rigidly severely limited the number of output sequences, so that individual rules were relaxed (see materials and methods section), and in particular the requirement for a set number of recurring motifs. Furthermore, even though an amphipathic, helical conformation was implicit in the design, a projection angle between successive side chains of 110° was also allowed. This is intermediate to an α-helix and a 3_{10} helix, which has a projection angle of 120° between successive residues. It has however been reported that 3_{10} helices in proteins can be distorted to have angles closer to 110°.[17] A change in the projection angle contributes to a variation in the amphipathicity and can result in a better separation of polar and hydrophobic residues into separate sectors, as observed in helical wheel projections (see Figure S1 in Supporting Information). In any case, natural helical AMPs seldom have an optimal amphipathicity, as it is usually only about 60% that of a perfectly amphipathic helix.[18] This may be required to limit cytotoxicity toward host cells, while adopting a slightly different conformation that improves amphipathicity when interacting with anionic bacterial membranes may improve potency.

DOI: 10.1021/acs.jmedchem.7b01831
J. Med. Chem. 2018, 61, 2924−2936

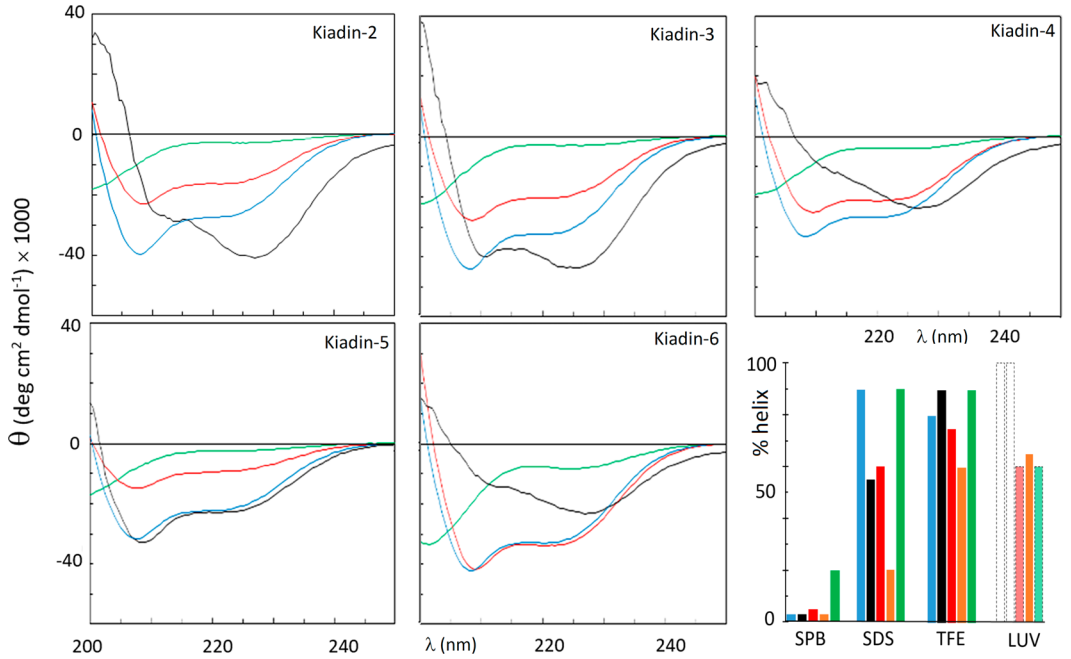

Figure 1. CD spectra of kiadin peptides under different conditions. Spectra are the accumulation of three scans carried out with 20 μM peptide in SPB (green line), 10 mM SDS in SPB (red line), 50% TFE (blue line), and anionic LUVs in SPB (PG:dPG 95:5, 0.4 mM phospholipid, black line). Inset bottom right shows the % helix content for kiadin-2 (blue box), kiadin-3 (black box), kiadin-4 (red box), kiadin-5 (orange box), and kiadin-6 (green box) in different environments. Note that in the presence of LUVs, the spectral shape deviates significantly from that of a canonical α-helix, so estimates are unreliable (shown as white dotted histograms).

The redesigned peptides had either a redistribution or increased number of Gly residues, consistent with the design rules (in particular iii, iv, and v; see materials and methods section) and the selectivity prediction algorithm. This was expected to increase the flexibility of the peptides and possibly also to affect their activity, based on previous reports.[13−16]

Peptide Structure. The effect of environment on the structure of kiadin peptides was determined by CD spectroscopy, as shown in Figure 1. As expected, spectra are consistent with random structures in 10 mM phosphate buffer (SPB), although kiadin-6 shows a weak band at >210 nm which may indicate some structuring. All peptides show a transition in their CD spectra to a shape that is characteristic of α-helices in the presence of 10 mM SDS or 50% TFE, conditions known to stabilize this conformation. TFE favors H-bond formation in helices, so peptides have similar helix content irrespective of the number of Gly residues in the sequence. In the presence of SDS micelles, a rough model of biological membranes, the amphipathic nature of the helix also plays a role and the degree of structuring is more varied (see Figure 1 inset and Table S1). Thus, the increased amphipathicity of kiadin-6 (μH^{rel} = 0.55) favors increased helicity with respect to kiadin-2 (μH^{rel} = 0.45), that of kiadin-4 (μH^{rel} = 0.73) helps maintain a similar helicity despite the presence of four Gly residues, while the poorly amphipathic kiadin-5 (μH^{rel} = 0.35) has a decreased helicity.

In the presence of anionic LUVs, the shape of the CD spectra for most peptides deviates significantly from that of a canonical α-helix (which normally shows well separated troughs at 208 and 222 nm and $\theta_{222}/\theta_{208} < 1$) to having a markedly deeper trough at ~225 nm (i.e., $\theta_{222}/\theta_{208} > 1$). For kiadin-5 only, the spectrum is less intense and unaltered, possibly indicating a different type of interaction with the membrane. There are different possible explanations for the altered CD spectra, one being the transition to a conformation more like a 3_{10} helix, which has been reported to result in a $\theta_{222}/\theta_{208}$ ratio of >1.[20] Another could be aggregation of helices to form bundles, as helix stacking has also been reported to result in a $\theta_{222}/\theta_{208}$ ratio of >1,[21] and this is particularly evident for helixes in transmembrane regions of proteins.[22] In any case, it is an indication that all peptides except kiadin-5 interact with the biological membrane in a manner that depends on their particular sequence and that this results in either a distortion of the canonical helical conformation or assembly into bundles. It should be noted that a similar effect has been reported for kiadin-1,[9] and also for unrelated designed or natural peptides rich in Gly residues, in the presence of LUVs.[23−25] However, it is observed only for LUVs composed principally of anionic phospholipids such as PG.

Antibacterial Activity. The antibacterial activity of kiadin peptides was assessed against the clinically relevant ESCAPE pathogens *E. coli*, *K. pneumoniae*, *P. aeruginosa*, *A. baumannii*, and *S. aureus*. Reference ATCC strains were assayed as well as multidrug-resistant clinical isolates (Table 2). Among the tested peptides, kiadin-2 was the most potent, in particular against Gram-negative opportunistic pathogens. Its MIC against reference ATCC and clinical isolates is generally similar. Kiadin-3 and kiadin-4, with an increased number of Gly residues in the sequences, showed a generally lower potency and a wider range of activities than kiadin-2, which was significantly reduced against some clinical isolates. However, this is not the only factor affecting activity, as kiadin-4 (4 Gly) still has an appreciable activity against ATCC microorganisms, while kiadin-5 (also 4 Gly) completely loses activity. It is likely that its particularly low amphipathicity (μH^{rel} = 0.36, Table 2) contributes to this, whereas the high amphipathicity of kiadin-4 (μH^{rel} = 0.73) allows it to maintain activity.

Kiadin-6, with one Gly residue but in a different position to kiadin-2, exhibited good activity against all ATCC strains but

DOI: 10.1021/acs.jmedchem.7b01831
J. Med. Chem. 2018, 61, 2924−2936

Table 2. Antimicrobial Activity of Kiadin Peptides Measured as MIC and MBC Values (μM) along with HC_{50} Values (μM) and Calculated Selectivity Index (SI)

	kiadin-2			kiadin-3			kiadin-4			kiadin-5			kiadin-6		
antimicrobial activity[a]	MIC	MBC	SI[c]	MIC	MBC	SI[c]	MIC	MBC	SI[c]	MIC	MBC	SI[c]	MIC	MBC	SI[c]
E. coli (ATCC 25922)	0.25–0.5	0.5–1	60–120	4	16	25 ± 2	8	16	2 ± 0.5	>64	>64		1–2	2–4	5–10
E.coli (c.i.)	4	8	7 ± 1	64	>64	<1	32–64	64	<1	>64	>64		32	32	<1
A. baumannii (ATCC 19606)	0.5–1	1	30–60	1–2	2	50–100	2	2	5 ± 1	>64	>64		2	2	5 ± 1
A. baumannii (c.i.)	0.5	1	60 ± 5	>64	>64	<1	32–64	64	<1	>64	>64		16–32	32	<1
K. pneumoniae (ATCC 13883)	2	2	15 ± 2	2–4	4	25–50	16	32	<1	>64	>64		2–4	4	2–6
K. pneumoniae (c.i.)	4	8	7 ± 1	8	16	12 ± 1	16	32	<1	>64	>64		16–32	32–64	<1
P. aeruginosa (ATCC 27853)	2	4	15 ± 2	8–16	16–32	6–12	8	16	2 ± 0.5	>64	>64		8–16	16	<1
P. aeruginosa (c.i.)	2–4	4	7–15	8–16	16	6–12	16–32	32	<1	>64	>64		32	32	<1
S. aureus (ATCC 25923)	8–16	8–16	2–4	16–32	32	3–6	16	32	<1	>64	>64		4	4	2.5 ± 0.5
S. aureus (c.i.)	4–8	8	4–8	16	16	6 ± 1	16	16–32	<1	>64	>64		2–4	4–8	2–6
hemolytic activity[b]															
HC_{50}	30 ± 3			100 ± 5			15 ± 2			nd			10 ± 1		

[a]MIC assays were carried out in 100% (v/v) MH broth using 1×10^6 cells/mL bacteria in the logarithmic phase; MBC assay (concentration resulting in >99.9% reduction in CFU). In both cases, presented are the mean values of two assays carried out in triplicate. ATCC codes are listed in Materials section. [b]Hemolysis assay, mean of three assays carried out in duplicate; HC_{50} values were the extrapolated point where 50% hemolysis occurs from the % lysis vs concentration curves. [c]Selectivity index calculated as HC_{50}/MIC.

showed decreased activity against Gram-negative clinical isolates. Conversely, it showed the best activity against the MRSA clinical isolate (MIC of 2−4 μM). In general, the MBC values obtained for this and other kiadin peptides was comparable to the MICs, suggesting their activity is bactericidal rather than bacteriostatic.

Considering structural aspects, it appears that the potency correlates more with the type of conformational changes that occur on membrane interaction rather than on the peptide helicity. Active peptides kiadin-2, -3, -4, and -6 show a more or less significant deviation from a canonical helical spectrum, suggesting the conformation is altered on membrane interaction, whereas the inactive kiadin-5 shows a canonical spectrum indicating a different type of interaction, consistent with MD studies (see below).

The antimicrobial activity of kiadins was assessed also in terms of bacterial growth inhibition of reference *E. coli* and *S. aureus* strains, in the presence of increasing peptide concentrations (Figure 2 and Figures S2 and S3). These assays are more sensitive than MIC, as they allow observation of inhibitory effects also at subtoxic concentrations. All peptides except kiadin-5 showed the capacity to inhibit growth at concentrations well below the MIC, even though the bacterial load was higher than in MIC assays (see materials and methods section). The inhibiting effect was quantified by determining IC_{50} values for the peptides (Figure 2, inset), and the trend is generally similar to that observed in MIC. For *E. coli* inhibition followed the trend kiadin-2 > kiadin-6 > kiadin-4 ≫ kiadin-5, although kiadin-3 bucks the trend, as it blocks growth over a 4 h period at just 0.5 μM concentration, more than 10-fold lower than the MIC. The trend with *S. aureus* is in line with the MIC: kiadin-6 > kiadin-2 > kiadin-3 > kiadin-4 ≫ kiadin-5. IC_{50} values are a somewhat higher than for *E. coli* but in any case significantly lower than the MIC

These data suggest that the peptides interact with the bacterial membrane and interfere with growth processes already at sublethal concentrations, but the bacteria can somehow eventually detoxify their membrane and continue growing so that the MIC values, recorded after overnight growth, are significantly higher than concentrations sufficient to block shorter term growth.

Bacterial Membrane Permeability. Given that amphipathic, helical AMPs generally act by disrupting bacterial membranes, causing toroidal pores or a general membrane disruption due to a detergent-like effect (carpet model),[26,27] we tested whether the kiadin peptides could permeabilize the membrane integrity of *E. coli* by the propidium iodide (PI) uptake assay. All peptides, except kiadin-5, showed a significant capacity to permeabilize the membrane in a time and concentration dependent manner (Figure 3). For comparison, melittin was used as positive control (at 5 μM). At peptide concentrations corresponding to the MIC value kiadin-3, -4, and -6 caused significant permeabilization (>80% PI+ cells) after just 15 min of treatment, and significant permeabilization was observed also at $^1/_2$ and $^1/_4$ the MIC. Only kiadin-5 did not cause any alteration in membrane permeability at any concentration or exposure time (<5% of PI-positive cells irrespective of exposure times). Significantly, the membrane permeabilization capacity did not correlate directly with the antibacterial potency, as kiadin-2, which has the generally lowest MIC, was apparently less effective at permeabilizing the membrane than kiadin-3, -4, and -6, considering the effect in terms of $^1/_4$, $^1/_2$, and 1-fold MIC (Figure 3A−C). Considering the concentration dependence of

DOI: 10.1021/acs.jmedchem.7b01831
J. Med. Chem. 2018, 61, 2924−2936

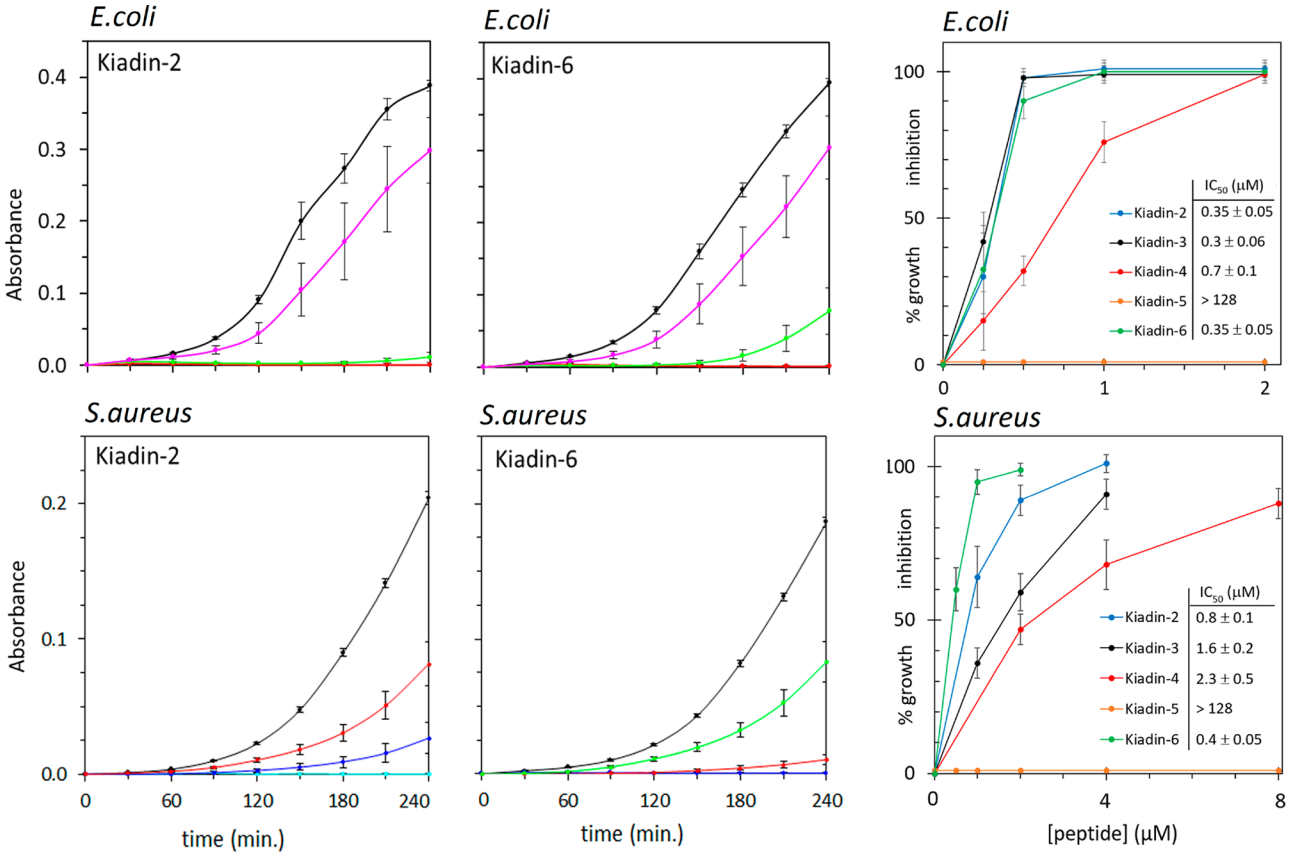

Figure 2. Effect of kiadins on bacterial growth kinetics. Growth curves for *E. coli* ATCC 25922 (top) or *S. aureus* ATCC 25923 (bottom) are shown after incubation with no peptide (black line), 0.25 (red line), 0.5 (green line), 1 (red line), 2 (blue line), 4 (light-blue line), and 8 (orange line) μM kiadin-2 and -6. Curves for other kiadins are shown in Figures S2 and S3. Results were obtained by measuring the absorbance at 620 nm for bacteria grown in full MHB. The % inhibition plots (left) were determined by comparing the OD values at 210 min for treated and untreated cells (see Materials section). The IC_{50} values were estimated from these plots as the concentrations resulting in 50% inhibition and are shown in the inset.

permeabilization (Figure 3D), kiadin-6 is more effective than kiadin-2, and kiadin-4 has a similar permeabilizing capacity.

Results can be summarized as follows: (a) kiadins act by permeabilizing the membrane quite rapidly and also at sub-MIC; (b) the extent of permeabilization depends on the sequence and does not necessarily correlate with potency. Explanations could be either that (i) a certain amount of membrane damage occurs already at sublethal concentration, but the bacteria can recover on the longer term (in line with growth inhibition studies), or (ii) subpopulations of bacteria are differentially refractory to permeabilization by the peptides at submic concentrations. Together with the variation in growth kinetics and antibacterial potency of the kiadins, results confirm that they have an overall lytic mode of action with sequence dependent differences.

AFM Images. To visualize the effect of kiadins on the *E. coli* membrane, AFM images were collected after exposure of bacterial cells to concentrations equivalent to the MIC and MBC (Figure 4), as compared to untreated cells. Images of bacteria treated with melittin and colistin were also obtained as examples of the effects of other types of lytic antimicrobial substances.[28,29] For this purpose, MIC and MBC values for colistin on *E. coli* ATCC 25922 were evaluated as described in materials and methods section and determined to be 0.5 μM. Melittin activity has been reported previously as 10 and 20 μM for MIC and MBC, respectively.[30]

Untreated cells have unperturbed surfaces and display pili and flagella. Bacteria treated with kiadin-2, -3, -4, and -6 at the MIC concentrations show clear signs of membrane alteration with bleb formation, surface indentations, and evidence of pores/cavities. These effects are even more marked after exposure to kiadins at the MBC concentrations, often with evidence of massive cell disruption/collapse and loss of pili/flagella. Only kiadin-5 did not apparently alter the membrane or affect pili/flagella even up to 128 μM.

The AFM images indicate a certain variation in the effects of kiadins, suggesting that they have subtly different modes of action. Kiadin-2 has a low MIC (0.25−0.5 μM), where at 0.25 μM only incipient damage is observed, although it possibly affects cell division at this concentration. At 0.5 μM, which is borderline MIC, more extensive damage is evident, while massive damage is evident at 1 μM. Effects of kiadin-6 at MIC (1−2 μM) and MBC (2−4 μM) are similar, and treated cells are blebbed with evidence of pores and indentations. Kiadin-3 caused little apparent membrane damage at its MIC (4 μM) but massive damage at the MBC (16 μM). Melittin and colistin also caused pili and flagellar loss at the MIC and MBC, with evidence of some cell wall alteration, but the damage is not nearly as substantial as in kiadin treated cells.

Taken together with the membrane permeabilization studies, carried out at comparable or lower concentrations ($^1/_4$ or $^1/_2$ the MIC), these studies suggest that the peptides act by a membrane permeabilising mechanism, which results in small scale membrane disruption at subtoxic concentrations (sufficient to allow PI to enter but not visible by AFM). They switch

DOI: 10.1021/acs.jmedchem.7b01831
J. Med. Chem. 2018, 61, 2924−2936

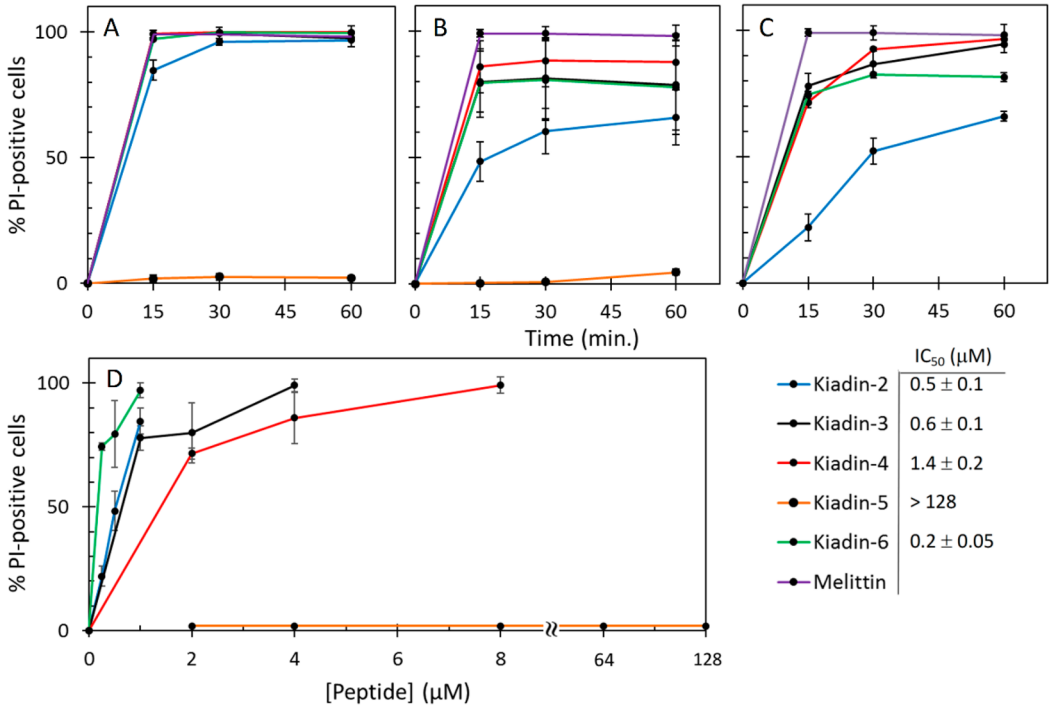

Figure 3. Evaluation of the effect of kiadins on *E. coli* membrane integrity. Tested peptides were (blue line) kiadin-2, (black line) kiadin-3, (red line) kiadin-4, (orange line) kiadin-5, and (green line) kiadin-6 as well as the reference permeabilising peptide melittin (purple line). (A-C) Bacterial cells (1×10^6 CFU/mL) were incubated for different incubation times with the peptides at a concentration equal to their MIC (A), $^1/_2$ MIC (B), or $^1/_4$ MIC (C) except kiadin-5, used at 128 μM (A) and 64 μM (B) (MIC values remained undetermined, >128 μM), and melittin, used at 5 μM. (D) The concentration dependence of permeabilization was determined after 15 min incubation. Data are expressed as the mean of % PI positive cells ± SEM of three independent experiments.

to a more massive damage (possibly membrane micellization, with blebbing and cavitation) at critical concentrations that correspond to the MIC. Bacteria can apparently recover from the first type of damage but not from the second.

Hemolytic Activity and Cyto/Genotoxicity. Lytic antimicrobial peptides tend to be potent and broad-spectrum but also somewhat cytotoxic to animal cells. For this reason, various types of cytotoxicity assays were performed with kiadins to determine whether these also show a sequence dependence. Figure 5 shows % hemolysis vs concentration, from which HC_{50} values could be determined (see Table 2). There is no apparent direct correlation between antimicrobial and hemolytic activity. Kiadin-2, the most potent antimicrobial, showed a relatively limited hemolytic activity, with a HC_{50} value of 30 μM (see Table 2), higher than kiadin-4 and kiadin-6 (10−15 μM) but lower than kiadin-3 (100 μM). By comparison, melittin has an HC_{50} value in the low micromolar range.[31] Kiadin-5 showed no hemolytic activity even at the highest concentrations used, which is in line with a general lack of activity of this peptide. This may in part be due to its lower hydrophobicity and amphipathicity (H and μH^{rel} in Table 1), leading to a different way of interacting with membranes that does not result in their perturbation, regardless of whether they are anionic bacterial or neutral host membranes.

Relating the HC_{50} value to the MIC, one can estimate a selectivity index (SI; see Table 2). It is acceptable for kiadin-2 and -3 (SI > 50 for some strains of *E. coli*, *A. baumannii*, and *S. aureus*) but generally low for kiadin-4 and -6. There is furthermore no direct correlation between cytotoxicity and number of Gly residues, but rather it seems to depend on a number of factors including helix-forming propensity (Table S1), amphipathicity (Table 1), and the particular arrangement of the hydrophobic sector (Figure S1).

HPBLs were exposed to kiadin-2 at increasing concentrations, up to 100 μM, to further verify its cyto/genotoxicity in comparison to colistin[9] and melittin[6] (Figure 6). No genotoxicity was observed, and the cell viability dropped in a statistically significant manner at 50 μM after 4 h (92 ± 6%) and 24 h (92 ± 8%) ($P < 0.05$). Even at 100 μM, viability was 89 ± 6% and 83 ± 9% ($P < 0.05$) after 4 and 24 h, respectively, and this is well above antimicrobially active concentrations. By comparison, melittin resulted in a significant drop in cell viability at submicromolar concentrations (e.g., 60% for 0.18 μM at 24 h, $P < 0.05$).[6]

MD Simulations. Antimicrobial and cytotoxic activity assays indicated that kiadins interact with and affect membranes in subtly different manners, which likely depend on their specific sequences. While an increased number of Gly residues was expected to contribute strongly in modulating helix stability, CD spectra (see Figure 1) indicated that the amphipathic arrangement of residues played an equally significant role. Furthermore, a deviation from the canonical spectra for α-helices was evident in the presence of anionic LUVs, suggesting some distortion of the helical conformation and/or membrane-mediated bundling.

To obtain further insight into how sequence features could affect conformation, we carried out extensive molecular dynamics simulations in different environments, including water, 30% v/v TFE, and membranes composed of DLPC. The initial structures for the peptides were obtained using the QUARK application, which suggested that all the peptides should have a substantially helical conformation [initial structures (t = 0 ns)

DOI: 10.1021/acs.jmedchem.7b01831
J. Med. Chem. 2018, 61, 2924−2936

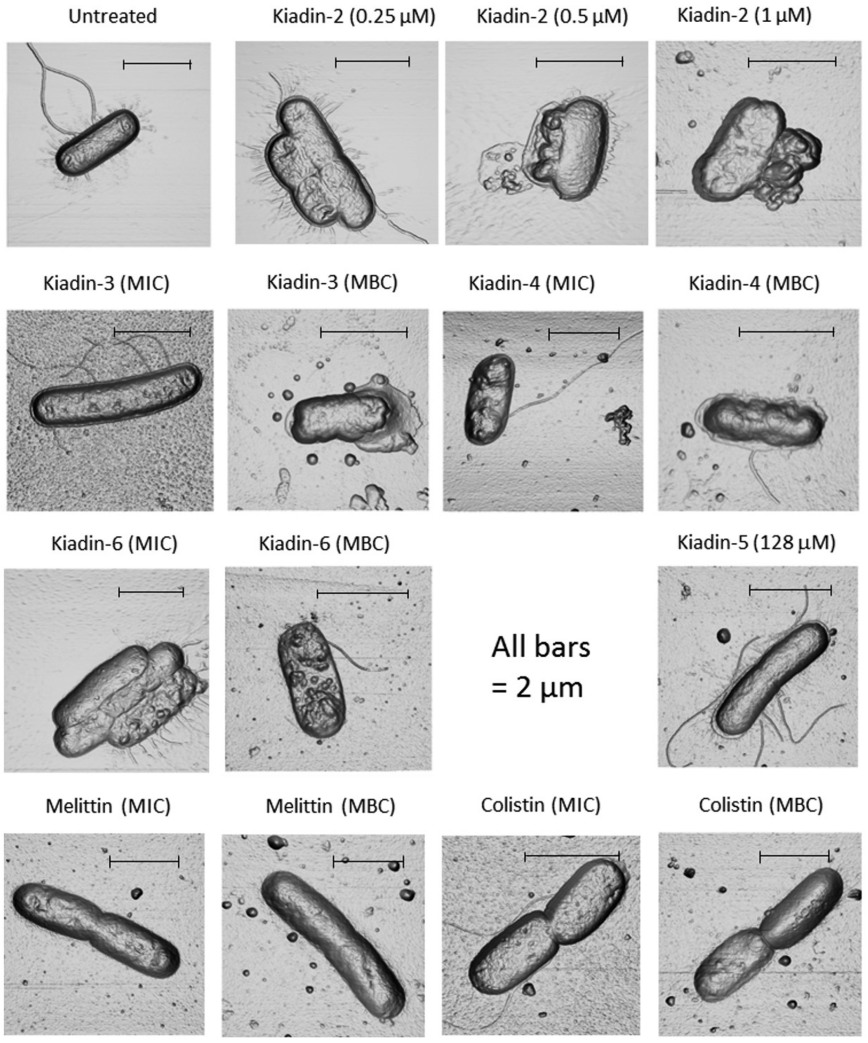

Figure 4. AFM images of *E. coli* in the presence of kiadins and other lytic antimicrobial peptides. All images are orthographic projections of three-dimensional images obtained from height data. Bacteria were exposed to the kiadins at concentrations equivalent to the MIC and MBC (generally 2 × MIC).

in Figures 7 and 8]. The peptides were then subjected to MD runs using the Gromacs package and the GROMOS (54a7) force field for peptides, lipids, and TFE and the SPC/E model for water (see materials and methods section). During these 120 ns runs the conformation was determined for each residue position, allowing monitoring of the evolution of the secondary structuring with time (see Figures S4 and S5 in Supporting Information). All five peptides showed unfolding of the initial α-helical conformation when immersed in water (Figures 7 and S4, top row). Kiadin-2 and -6 retain about 60% of residues with this conformation. Kiadin-3 retains about 40%, while kiadin-4 and -5 lose it substantially (calculated as an average over 120 ns simulation time). This suggests that an increased Gly content contributes to peptide unfolding in aqueous solution and defines regions of instability, which for kiadin-2 and kiadin-3 are near the C-terminal end, whereas for kiadin-6 it is more in the central region, preceding the Gly residue.

In the presence of TFE, the initial α-helical structure was stabilized and substantially preserved during the MD runs (Figure 7, middle row, and Figure S4 bottom row). Kiadin-5, with 4 Gly residues, had a low α-helicity, with the most visible fluctuations. Kiadin-4, also with 4 Gly, behaved more similarly to kiadin-3, with only 2 Gly, suggesting that the effect of the Gly residues is position and sequence dependent. Furthermore, kiadin-4 adopts the most amphipathic helical structure in its initial conformation, while kiadin-5 the least (see Table 2 and Figure S1 in Supporting Information).

Taken together, the MD simulations are in quite good agreement with the CD measurements (see Table S1 in Supporting Information), even providing an explanation for the increased helix content of kiadin-6 in aqueous environment, possibly due to internally stacked helical segments. When immersed in the hydrophobic core of the membrane (see Figure 7, bottom row), the peptides preserved their helical conformation and adopt energetically favorable contacts, exposing hydrophobic residues to the lipids acyl-chain and, by tilting, bringing the positively charged head of Lys side chains in contact with the zwitterionic lipid headgroups (snorkel effect). Only kiadin-5 did not conform to this process, since it remained vertical with unfolded termini reaching to the headgroups on each side of the membrane.

Finally, we simulated what would happen to a helical peptide placed close to, and with axis parallel to, the membrane surface (see Figure 8 and Figure S5 bottom row) to probe peptide propensity for binding to the surface and possible insertion path into the bilayer. We found that the unfolding rate has a

DOI: 10.1021/acs.jmedchem.7b01831
J. Med. Chem. 2018, 61, 2924−2936

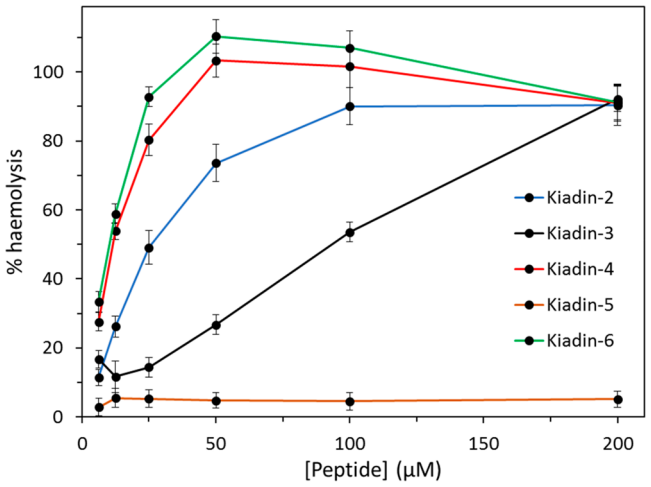

Figure 5. Hemolytic activity of kiadins. Human erythrocytes were treated with kiadins at increasing concentrations in PBS: kiadin-2 (points on blue line), kiadin-3 (points black line), kiadin-4 (points on red line), kiadin-5 (points on organge line), kiadin-6 (points on green line). Hemolysis was determined by measuring the absorbance of the supernatant at 450 nm after 1 h incubation of erythrocytes with each peptide at 37 °C, and results were compared to the values achieved by treatment with 1% Triton X-100 (considered to be 100% permeabilising). Data are expressed as mean values ± SE of three independent experiments performed in duplicate.

strong impact on these binding events, so that peptides with greater conformational stability in water make a stronger contact with the membrane surface. Only kiadin-5 completely unfolds and adopts an extended conformation on the membrane surface. Kiadin-2 and especially kiadin-6 approach the membrane with the helical axis remaining parallel to the surface, thus preserving the amphipathic helical structure. One could suppose that a next step would be to flip the hydrophobic sector into the lipid bilayer. Kiadin-3 and -4 instead adopt more vertical positions contacting with the positively charged N-terminus.

In conclusion, differences in the number and position of Gly, but likely also other residues, translate into specific amphipathic helical conformations and affect the propensity of peptides to adopt this conformation in different environments. This affects their capacity to interact with biological membranes and likely affects how they then insert into the membrane and the membrane-bound conformation they adopt.

CONCLUSIONS

Applying different types of design criteria allowed preparation of a self-consistent family of AMPs, the kiadins, with quite variable antimicrobial potency and selectivity that could be related to specific conformational characteristics and explained also using MD simulations. One common feature of the peptides is that they did not seem to interact with anionic biological membranes as canonical lone amphipathic helices but rather as distorted and/or bundled helices. Furthermore, while it had been expected that potency and selectivity should correlate with the number of Gly residues present in the sequence, providing structural flexibility, it was evident that the amphipathic arrangement of residues played an equally important role. In particular, a shallow hydrophobic sector composed mainly of Ala residues (e.g., kiadin-5) promotes unfolding and reduces interaction with the membrane, abrogating any type of activity. Conversely, a symmetric amphipathic arrangement with a hydrophobic sector clustering long aliphatic residues in its center (kiadin-4) promotes membrane interaction and insertion and consequently both antimicrobial and cytotoxic activity, regardless of helix flexibility. Modulating the amphipathic arrangement and flexibility allowed design of sequences that resulted in broad-spectrum antimicrobial activity while limiting cytotoxicity, as seen for kiadin-2. In this respect, it appears that the design procedure based on modification of a natural but poorly active peptide such as PGLa-H was more successful than ab initio design based on general rules derived from a training set of natural peptides, which failed to produce antimicrobial activity (kiadin-5) or to limit cytotoxicity (kiadin-4 and -6). However, it did provide useful information that may be used to refine the design process, particularly considering how spectroscopic, microbiological, and MD methods converged to provide explanations for the different behavior of peptides.

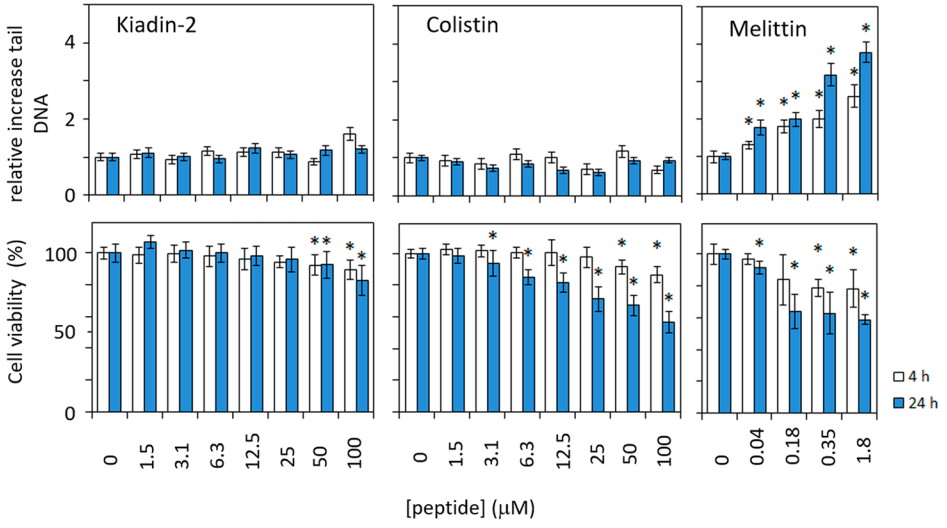

Figure 6. Cell viability (cytotoxicity) and DNA damage (genotoxicity) in HPBLs after exposure to kiadin-2. Cells were exposed to 0, 1.56, 3.13, 6.25, 12.5, 25, 50, and 100 μM for 4 and 24 h and subsequently evaluated by differential staining with acridine-orange (AO) and ethidium bromide (EtBr) and by the alkaline comet assay. Cell viability was determined by scoring 100 cells per repetition, while the % of tail DNA (as comet assay parameter) was determined in 100 nuclei per slide. Viability is presented as % of the corresponding controls, and genotoxicity is presented as mean % increase of DNA in comet tail relative to control cells. *Statistically significant ($P < 0.05$).

DOI: 10.1021/acs.jmedchem.7b01831
J. Med. Chem. 2018, 61, 2924−2936

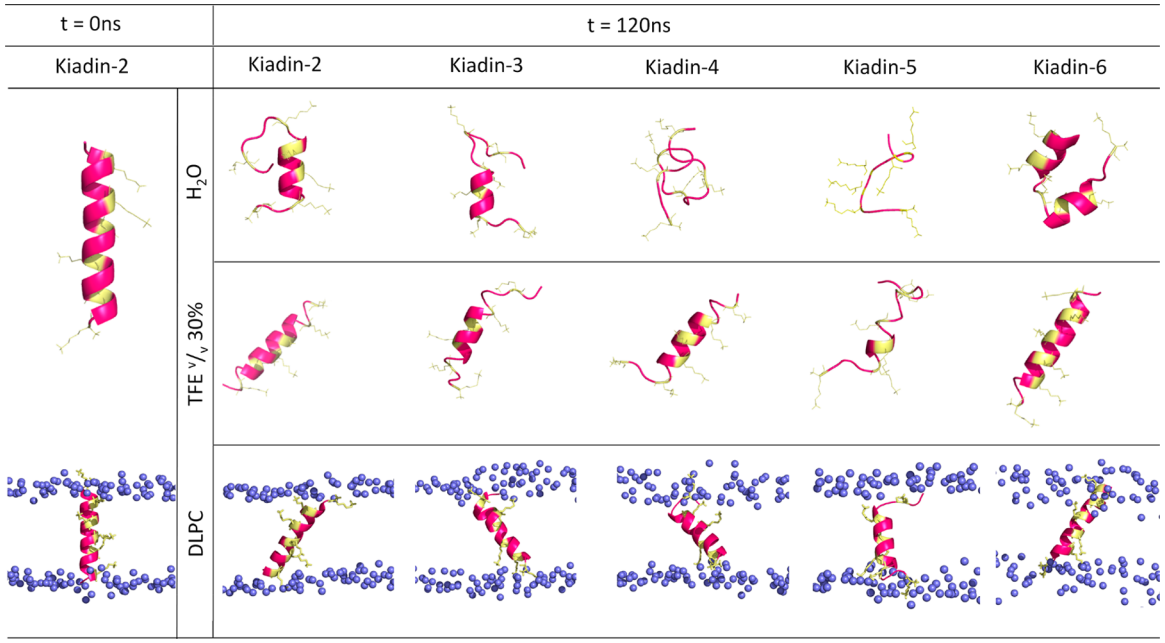

Figure 7. Molecular dynamics simulation of kiadin peptides. MD was carried out in an aqueous environment in the presence of 30% v/v TFE or on peptides placed within a DLPC membrane. All peptide starting structures were helical structures as produced by the Quark tool (that of kiadin-2 in water or inserted into DPLC bilayer is shown on the left as an example). The peptides were then subjected to 120 ns of MD as described, and the final structures are then shown. Peptides are represented as ribbon models with the hydrophobic residues in magenta and polar ones in yellow. Lys residue side chains are also shown as yellow stick representations. Only the membrane phospholipid phosphate groups are shown as blue spheres.

Another interesting aspect of the mode of action of kiadins is that while activity depends on the capacity to interact with and permeabilize bacterial membranes, it does so in a subtle manner. Potency did not necessarily correlate with permeabilising capacity but rather with the capacity to persist in the bacterial membrane leading to macroscopic damage of the bacterial cell wall. Taken together, our findings suggest some kiadins, particularly kiadin-2, can be further evaluated as leads for a new generation of antibiotics with limited host cell toxicity and active against multidrug resistant bacterial strains. This, however, is subject to further in vitro and in vivo testing. In any case, information on how structural modifications and amphipathic arrangement of residues affect peptide potency can be useful to improve design algorithms which may help the successful development of AMP analogues with improved potency and bioavailability for clinical use, cosmetics, or biomedical coatings.

EXPERIMENTAL SECTION

Materials. Acridine orange (AO), ethidium bromide (EtBr), histopaque, low and normal melting point agaroses, propidium iodide (PI), phosphatidylglycerol were from Sigma (St. Louis, MO, USA). Diphosphatidylglycerol was from Avanti Polar Lipids (Alabaster, AL, USA). Heparinized vacutainer tubes were from Becton Dickinson (Franklin Lakes, NJ, USA). Mueller−Hinton broth and agar were from Biolife (Milan, Italy). All other reagents used were laboratory-grade chemicals from Kemika (Zagreb, Croatia).

Peptide Design and Synthesis. The peptide sequence of kiadin-2 was based on that of kiadin-1, itself derived from the tandem repeat of the short natural peptide PGLa-H.[9] For kiadin-2, Val[5] and Gly[15] were simply inverted, and for kiadin-3, Gly was placed in both positions 5 and 15, as the number and position of Gly residues in helical peptides have been shown to affect potency and selectivity.[14,16] Kiadin-4, -5, and -6 were designed ab initio by applying a set of specific rules[11] that required the following:

(i) a length of 20 residues;
(ii) a charge of +7;
(iii) for any given residue, that the successive amino acids should be from among the most common successors in a training set of known anuran AMPs;
(iv) that residues spaced i, $i + 3$ or i, $i + 4$ apart in the sequence be matched so that they form motifs that are frequent in the training set;
(v) that there is a set lower limit "n" for the X^i---X^{i+3} and X^i---X^{i+4} motifs (where X = Lys in both positions or where X = Gly and/or Ala in both positions);
(vi) the sequence has a helical conformation (angle α between successive residue side chains is 100°) and the helix has an amphipathic nature in a helical wheel projection (good separation of hydrophobic and polar residues);
(vii) the peptide should have a D-descriptor value (a selectivity descriptor based on hydrophobicity)[11,32] that predicts a high selectivity index (SI) when using the Mutator algorithm,[33] a QSAR tool for AMP design based on a training set of anuran peptides with known antimicrobial and cytotoxic activities.

Applying these rules too strictly however reduced sequence variability to peptides composed effectively only of K, I, A, and G. Relaxing rule v by reducing the required minimum number of X^i---X^{i+3} and X^i---X^{i+4} motifs resulted in kiadin-4. Then relaxing rule vi so α could also be 110° resulted in kiadin-5. Further relaxing rules iii and iv resulted in kiadin-6.

Peptides were obtained from GenicBio Limited (Shanghai, China) as the C-terminally amidated forms, at >98% purity as confirmed by RP-HPLC and mass spectrometry. Chromatographic separation was achieved on a reversed-phase Phenomenex Gemini-NX column (C18, 5 μm, 110 Å, 4.6 mm × 250 mm) using a 25−50% acetonitrile/0.1% TFA gradient in 25 min at a 1 mL/min flow rate (see Figure S6). Stock solutions were prepared by dissolving accurately weighed aliquots of peptide in doubly distilled water, and the concentrations were further verified by using the extinction coefficients at 214 nm, calculated as described by Kuipers and Gruppen.[34]

Preparation of Liposomes. LUVs (large unilamellar vesicles) were prepared as described by Morgera et al.[35] Briefly, dry phosphatidylglycerol and diphosphatidylglycerol (PG:dPG 95:5 w/w) were dissolved in chloroform/methanol (2:1) solution, then evaporated

DOI: 10.1021/acs.jmedchem.7b01831
J. Med. Chem. 2018, 61, 2924−2936

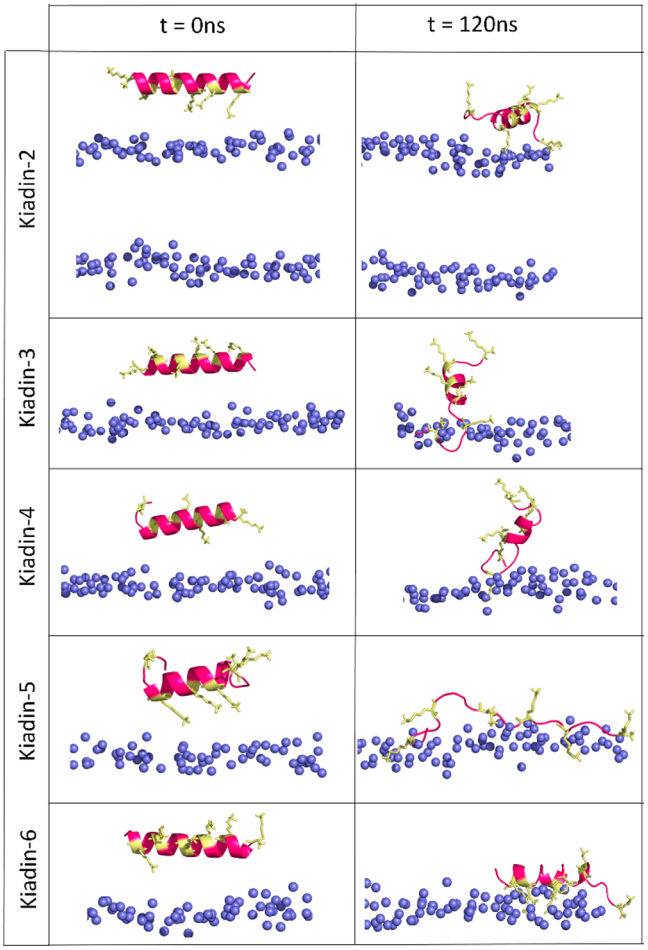

Figure 8. Molecular dynamics simulation of kiadins on the surface of a DLPC membrane. Starting structures were produced by the Quark tool and then placed close to, and parallel to, the membrane surface. The initial structure is shown on the left. They were then subjected to 120 ns of MD as described, and the final structure is then shown on the right. Except for kiadin-2, only the outer leaflet of the DPLC bilayer is shown, and only the membrane phospholipid phosphate groups are shown as blue spheres. Peptides are represented as ribbon models with the hydrophobic residues in magenta and polar ones in yellow. Lys residue side chains are also shown as yellow stick representations.

using a dry nitrogen stream and vacuum-dried for 24 h. The liposome cake was resuspended in 1 mL of sodium phosphate buffer (SPB) to a concentration of 5 mM phospholipid and spun for 1 h at 40 °C. The vesicles were then subjected to several freeze−thaw cycles before passing through a miniextruder (Avanti Polar Lipids, Alabaster, AL, USA) through successive polycarbonate filters with 1, 0.4, and 0.1 μm pores and resuspended to a final phospholipid concentration of 0.4 mM. On the basis of the bilayer membrane surface area of a ∼100 nm liposome and area of a phospholipid headgroup (∼0.7−1 nm^2),[18] the concentration of liposomes is about 5 nM.

Circular Dichroism. CD spectra were obtained on a J-710 spectropolarimeter (Jasco, Tokyo, Japan) and are accumulation of three scans. They were measured in (a) SPB solution, (b) 50% TFE in SPB, (c) sodium dodecyl sulfate micelles (10 mM SDS in SPB), or (d) anionic LUVs (PG:dPG 95:5) in SPB. The % helix content was determined as $[\theta]^{222}/[\theta]^{\alpha}$, where $[\theta]^{222}$ is the measured molar per residue ellipticity at 222 nm under any given condition and $[\theta]^{\alpha}$ is the molar ellipticity for a perfectly formed α helix of the same length, estimated as described by Chen et al.[36]

Bacterial Strains and Antibacterial Assays. The in vitro antibacterial activity was tested against standard laboratory strains from the American Type Culture Collection (ATCC, Rockville, MD, USA) including *S. aureus* ATCC 29213, *E. coli* ATCC 25922, *K. pneumoniae* ATCC 13883, *A. baumannii* ATCC 19606, and *P. aeruginosa* ATCC 27853. Multiple drug resistant clinical isolates for all these bacterial species were obtained from different wards of University Hospital Centre Split, Croatia. Their origin, antibiograms, and characterization of resistance determinants were described previously.[9]

Antimicrobial activity was assessed using the microdilution method according to EUCAST[37] and performed in 96-well microtiter plates as previously described.[9] In brief, an aliquot of overnight grown bacteria was cultured in fresh MHB to the mid exponential phase, added to serial dilutions (64−0.0625 μM) of peptides to a final load of 5 × 10^5 CFU/mL in 100 μL per well, and incubated at 37 °C for 18 h. MIC was taken as the lowest concentration of the peptide showing no visually detectable bacterial growth (consensus of three independent experiments performed in triplicate). For determination of minimal bactericidal concentration (MBC), 4 μL aliquots (corresponding to about 2000 CFU of initial inoculum) were taken from the wells corresponding to MIC, 2 × MIC, and 4 × MIC and then plated on MH agar plates. After incubation for 18 h at 37 °C, the MBC value was recorded as the concentration causing ≥99.9% of killing of the start inoculum.

The effect of kiadin peptides on *E. coli* ATCC 25922 and *S. aureus* ATCC 25923 was also assessed by a growth kinetics assay, as described.[13] Briefly, the bacterial growth curves were obtained using mid log phase bacteria at 1 × 10^6 CFU/mL per 200 μL per well in MHB, in the presence of increasing peptide concentrations, monitoring the optical density (OD) at 620 nm every 10 min at 37 °C for 4 h in a microplate reader with intermittent shaking (Tecan Trading AG, Männedorf, Switzerland). Experiments were carried out twice, in triplicate, and results are expressed as the mean ± SEM. IC_{50} values were determined by plotting % inhibition at 210 min vs peptide concentration.

Membrane Integrity Assay. The integrity of bacterial cell membrane of *E. coli* ATCC 25922 was assessed by measuring the PI uptake in flow cytometry, using a Cytomics FC 500 instrument (Beckman-Coulter, Inc., Fullerton, CA, USA). Mid log phase bacterial cultures, diluted to 1 × 10^6 CFU/mL in Mueller−Hinton Broth (MHB), were incubated at 37 °C for different times with kiadin peptides at $^1/_4$, $^1/_2$, and 1 × their MIC values. PI was then added to a final concentration of 10 μg/mL (15 μM). Data analysis was performed with the FCS Express3 software (De Novo Software, Los Angeles, CA, USA).

AFM Imaging. *E. coli* ATCC 25922 was grown overnight in MHB with shaking at 100 rpm at 37 °C, and 200 μL was added to 4800 μL of fresh broth and grown to the mid logarithmic phase (∼150 × 10^6 CFU/mL). Kiadin peptides were then added to 0.5 mL of this suspension, to their MBC and MIC concentrations, and incubated with shaking at 100 rpm at 37 °C for 1 h. Control samples were prepared in the same way but without the kiadin treatment. All experiments were conducted in triplicate for each concentration of each peptide. To obtain good bacterial adhesion, circular glass slides were first coated with Cell-Tak solution (Corning, NY, USA) prepared according to Louise Meyer et al.[38] An amount of 20 μL of this solution was applied to each slide and left at room temperature for 30 min before rinsing in deionized water. After thorough drying, 10 μL of the treated cell culture was placed on the prepared surfaces, left for 20 min, rinsed with sterilized deionized water to remove loose bacteria, and left to dry before imaging. AFM imaging was carried out in contact mode, under ambient conditions, using a Bruker Multimode 3 (Digital Instruments, USA) with a 0.12 N/m silicon nitride probe (Bruker AFM probes USA, DNPS-10). Scan rates were kept between 1 and 3 Hz, and the image resolution was 512 pixels per line. Imaging was carried out in air as this has been shown to be a good method to obtain high resolution of the bacteria surface morphology.[39] Analysis of the obtained images was carried out with Gwyddion.

Cyto/Genotoxicity Assays. Peripheral blood samples were drawn from young healthy, nonsmoking male donors into vacutainers containing anticoagulant under aseptic conditions. Subjects gave informed consent to participate in these studies, which were approved by the Ethics Committee and observed the ethical principles of the Declaration of Helsinki. Leukocytes and erythrocytes were isolated as

DOI: 10.1021/acs.jmedchem.7b01831
J. Med. Chem. 2018, 61, 2924−2936

appropriate for different assays. Each experiment was repeated three times.

The effect of peptides on hRBC was determined by the hemolysis assay as described previously.[9] Briefly, hemoglobin release was monitored for 0.5% (v/v) whole blood suspensions in PBS, at 450 nm using an ELx808 Ultra Microplate Reader (BioTek, Inc., Winooski, VT, USA). Total lysis (100% hemolysis) was determined by the addition of 1% (v/v) Triton X-100. Three independent evaluations were carried out in duplicate, and the HC_{50} value was the peptide concentration estimated to produce 50% hemolysis.

Cell viability (cytotoxicity) was determined by fluorescence microscopy after differential staining (AO/EtBr) of human peripheral blood leukocytes (HPBLs) as described in detail previously.[9] Briefly, after the treatment, cells were isolated by histopaque density gradient centrifugation and stained with AO/EtBr. A total of 100 cells per repetition were examined with an epifluorescence microscope (Olympus BX51, Tokyo, Japan). Cytotoxicity was evaluated by determining the percentage of live and dead cells based on their appearance.

DNA damage (genotoxicity) was determined by the alkaline comet assay.[40,41] Briefly, after the treatment, whole blood was imbedded into agarose gels, and after solidifying, the cells were lysed using 2.5 M NaCl, 100 mM $EDTANa_2$, 10 mM Tris, 1% sodium sarcosinate, 1% Triton X-100, 10% DMSO, pH 10, at 4 °C. The slides were then placed into alkaline solution (300 mM NaOH, 1 mM $EDTANa_2$, pH 13) for 20 min at 4 °C and subsequently electrophoresed for another 20 min at 1 V/cm. Finally, the slides were neutralized using 0.4 M Tris buffer (pH 7.5), stained with EtBr (10 μg/mL) and analyzed at 250× magnification under an epifluorescence microscope (Zeiss, Göttingen, Germany) using an image analysis system (Comet Assay II; Perceptive Instruments Ltd., Haverhill, Suffolk, U.K.). One-hundred randomly captured comets from each slide were examined, and the percent of tail DNA was used to measure the level of DNA damage.

Results were evaluated using the Statistica 13 program (StaSoft, Tulsa, OK, USA). HPBL viability was evaluated by χ^2-test. In order to normalize the distribution and equalize the variances of the comet assay data, a logarithmic transformation was applied. Multiple comparisons between groups were carried out by means of ANOVA on log-transformed data. Post hoc analyses of differences were obtained by using the Scheffé test. Results are presented either as the mean ± SD (standard deviation of the mean) or as the mean ± SE (standard error of the mean). P values less than 0.05 were considered to be statistically significant.

Molecular Modeling. Molecular dynamics simulations were carried out in three different environments: water, a TFE/water mixture, or neutral, solvated DLPC membrane. The QUARK, template-free protein structure predictor was used to defined the initial coordinates.[42] Predicted structures with the highest score were in all cases α-helical. The Gromacs program version 5.0.7. was then used for the simulations,[43] with the GROMOS (54a7) force field for peptides, lipids, and TFE and SPC/E model for water.[44−46] Peptide charge was defined for pH 7, with a neutral, amidated C-terminus. Four different simulations were carried out for each peptide. (1) It was immersed in an octahedral box with at least 4000 water molecules. (2) It was immersed in a cubic box with a 10 M solution of TFE (ranging from 417 TFE + 4167 H_2O for kiadin-5 to 691 TFE + 6913 H_2O for kiadin-2, corresponding to ∼30% v/v). (3) It was immersed in the central part of an equilibrated DLPC lipid bilayer (∼110 lipid molecules per leaflet solvated in ∼11 000 water molecules) using an InflateGRO method similar to known procedures.[47,48] (4) It was placed in the aqueous layer parallel to, and ∼1.6 nm distant from, the surface of an equilibrated DLPC lipid bilayer, as described above.

Seven Cl^- counterions were added to neutralize peptide charges, and a temperature annealing procedure was used to equilibrate the system to the reference temperature T = 310 K and pressure p = 1 atm,[43] ensuring that lipids are in the fluid phase (T_M = 272 K for DLPC).[25] During equilibration, a position restraint algorithm was used to fix peptide atoms and preserve their helical structure. Production runs of 120 ns were then performed in isothermal−isobaric (constant NpT) ensemble (using the modified Berendsen thermostat and Parrinello−Rahman barostat, 0.1 ps time constant for the temperature, 2.0 ps for the pressure, and compressibility equal to 4.5×10^{-5} bar).[49,50] The leapfrog integrator time step was fixed at 2 fs, and the bonds were handled by the LINCS option.[51] The particle-mesh Ewald method was used for calculation of the electrostatic interaction, and the van der Waals cutoff was set to 1.0 nm.[52]

Analysis of the resulting secondary structuring was carried out with Gromacs[43] utilities and the DSSP program.[53] Molecular visualization was by PyMOL.[54]

Data generated during and/or analyzed during the current study are available from authors on reasonable request.

■ ASSOCIATED CONTENT

Supporting Information

The Supporting Information is available free of charge on the ACS Publications website at DOI: 10.1021/acs.jmedchem.7b01831.

Training set of peptides with measured MIC (*E. coli*) and HC_{50} values; helical content of peptides in different environments and helical wheel projections; effect of peptides on *E. coli* and *S. aureus* growth kinetics; and molecular dynamics simulation of peptides in an aqueous environment, in the presence of 30% v/v TFE, and when placed within and on the surface of the DLPC membrane (PDF)

■ AUTHOR INFORMATION

Corresponding Author

*Phone: 00385-21-619-281. E-mail: amaravic@pmfst.hr.

ORCID

Ana Maravić: 0000-0001-5235-6656

Author Contributions

T.R. carried out antimicrobial assays, CD measurements, and hemolysis assays, and wrote the manuscript. A.T. and A.M. helped plan the experiments, analyzed data, and wrote the manuscript. M.B. carried out flow cytometric and growth kinetics analyses. D.J. designed some peptides, analyzed data, and helped write the manuscript. D.V. created the computational design algorithms. L.K. set up and carried out the AFM experiments. N.I. assisted with antimicrobial and hemolysis assays. G.G. carried out cyto- and genotoxicity assays. M.T. and I.G.-B. provided strains, determined antibiograms, and helped with execution and analysis of antimicrobial activity assays. L.Z. planed MD experiments, analyzed data, and helped write the MD part of the manuscript. Y.S. set up, carried out, and analyzed MD experiments. All authors reviewed and discussed the results.

Notes

The authors declare no competing financial interest.

■ ACKNOWLEDGMENTS

This work was supported by the Croatian Science Foundation (Grants 8481 and 4514). L.Z. thanks Prof. Alan Mark and Dr. David Poger (Molecular Dynamics Group, University of Queensland, Australia) for the help in preparation of the lipids systems.

■ ABBREVIATIONS USED

AMP, antimicrobial peptide; AO, acridine orange; AFM, atomic force microscopy; CD, circular dichroism; CFU, colony forming unit; diC12, DLPC, 1,2-dilauroyl-*sn*-glycero-3-phosphocholine; DMSO, dimethyl sulfoxide; dPG, diphosphatidylglycerol; EtBr, ethidium bromide; EDTA, ethylenediaminetetraacetic acid; ESBL, extended-spectrum β-lactamase; HPBL,

DOI: 10.1021/acs.jmedchem.7b01831
J. Med. Chem. 2018, 61, 2924−2936

human peripheral blood leukocyte; LMP, low melting point; LUV, large unilamellar vesicle; MHB, Mueller−Hinton broth; MD, molecular dynamics; NMP, normal melting point; PG, phosphatidylglycerol; PI, propidium iodide; SDS, sodium dodecyl sulfate; SPB, sodium phosphate buffer; TFA, trifluoroacetic acid; TFE, trifluoroethanol

REFERENCES

(1) World Health Organization. Global Priority List of Antibiotic-Resistant Bacteria to Guide Research, Discovery, and Development of New Antibiotics. http://www.who.int/medicines/publications/global-priority-list-antibiotic-resistant-bacteria/en/ (accessed May 7, 2017).

(2) Liu, Y.-Y.; Wang, Y.; Walsh, T. R.; Yi, L.-X.; Zhang, R.; Spencer, J.; Doi, Y.; Tian, G.; Dong, B.; Huang, X.; Yu, L.-F.; Gu, D.; Ren, H.; Chen, X.; Lv, L.; He, D.; Zhou, H.; Liang, Z.; Liu, J.-H.; Shen, J. Emergence of Plasmid-Mediated Colistin Resistance Mechanism MCR-1 in Animals and Human Beings in China: A Microbiological and Molecular Biological Study. *Lancet Infect. Dis.* **2016**, *16* (2), 161−168.

(3) Park, S.-C.; Park, Y.; Hahm, K.-S. The Role of Antimicrobial Peptides in Preventing Multidrug-Resistant Bacterial Infections and Biofilm Formation. *Int. J. Mol. Sci.* **2011**, *12* (12), 5971−5992.

(4) Baltzer, S. A.; Brown, M. H. Antimicrobial Peptides − Promising Alternatives to Conventional Antibiotics. *J. Mol. Microbiol. Biotechnol.* **2011**, *20* (4), 228−235.

(5) Hancock, R. E. W.; Sahl, H.-G. Antimicrobial and Host-Defense Peptides as New Anti-Infective Therapeutic Strategies. *Nat. Biotechnol.* **2006**, *24* (12), 1551−1557.

(6) Gajski, G.; Domijan, A.-M.; Žegura, B.; Štern, A.; Gerić, M.; Novak Jovanović, I.; Vrhovac, I.; Madunić, J.; Breljak, D.; Filipič, M.; Garaj-Vrhovac, V. Melittin Induced Cytogenetic Damage, Oxidative Stress and Changes in Gene Expression in Human Peripheral Blood Lymphocytes. *Toxicon* **2016**, *110*, 56−67.

(7) Mauro, N.; Schillaci, D.; Varvarà, P.; Cusimano, M. G.; Geraci, D. M.; Giuffrè, M.; Cavallaro, G.; Maida, C. M.; Giammona, G. Branched High Molecular Weight Glycopolypeptide With Broad-Spectrum Antimicrobial Activity for the Treatment of Biofilm Related Infections. *ACS Appl. Mater. Interfaces* **2018**, *10* (1), 318−331.

(8) Takahashi, H.; Nadres, E. T.; Kuroda, K. Cationic Amphiphilic Polymers with Antimicrobial Activity for Oral Care Applications: Eradication of *S. Mutans* Biofilm. *Biomacromolecules* **2017**, *18* (1), 257−265.

(9) Rončević, T.; Gajski, G.; Ilić, N.; Goić-Barišić, I.; Tonkić, M.; Zoranić, L.; Simunić, J.; Benincasa, M.; Mijaković, M.; Tossi, A.; Juretić, D. PGLa-H Tandem-Repeat Peptides Active against Multidrug Resistant Clinical Bacterial Isolates. *Biochim. Biophys. Acta, Biomembr.* **2017**, *1859* (2), 228−237.

(10) Fjell, C. D.; Hiss, J. A.; Hancock, R. E. W.; Schneider, G. Designing Antimicrobial Peptides: Form Follows Function. *Nat. Rev. Drug Discovery* **2012**, *11*, 37−51.

(11) Juretić, D.; Vukičević, D.; Ilić, N.; Antcheva, N.; Tossi, A. Computational Design of Highly Selective Antimicrobial Peptides. *J. Chem. Inf. Model.* **2009**, *49* (12), 2873−2882.

(12) Novkovic, M.; Simunic, J.; Bojovic, V.; Tossi, A.; Juretic, D. DADP: The Database of Anuran Defense Peptides. *Bioinformatics* **2012**, *28* (10), 1406−1407.

(13) Ilić, N.; Novković, M.; Guida, F.; Xhindoli, D.; Benincasa, M.; Tossi, A.; Juretić, D. Selective Antimicrobial Activity and Mode of Action of Adepantins, Glycine-Rich Peptide Antibiotics Based on Anuran Antimicrobial Peptide Sequences. *Biochim. Biophys. Acta, Biomembr.* **2013**, *1828* (3), 1004−1012.

(14) Zelezetsky, I.; Pag, U.; Sahl, H.-G.; Tossi, A. Tuning the Biological Properties of Amphipathic α-Helical Antimicrobial Peptides: Rational Use of Minimal Amino Acid Substitutions. *Peptides* **2005**, *26* (12), 2368−2376.

(15) Liu, L.; Fang, Y.; Wu, J. Flexibility Is a Mechanical Determinant of Antimicrobial Activity for Amphipathic Cationic α-Helical Antimicrobial Peptides. *Biochim. Biophys. Acta, Biomembr.* **2013**, *1828* (11), 2479−2486.

(16) Sani, M.-A.; Saenger, C.; Juretic, D.; Separovic, F. Glycine Substitution Reduces Antimicrobial Activity and Helical Stretch of DiPGLa-H in Lipid Micelles. *J. Phys. Chem. B* **2017**, *121* (18), 4817−4822.

(17) Geetha, V. Distortions in Protein Helices. *Int. J. Biol. Macromol.* **1996**, *19* (2), 81−89.

(18) Tossi, A.; Sandri, L.; Giangaspero, A. Amphipathic, α-Helical Antimicrobial Peptides. *Biopolymers* **2000**, *55* (1), 4−30.

(19) Tossi, A.; Sandri, L.; Giangaspero, A. New Consensus Hydrophobicity Scale Extended to Non-Proteinogenic Amino Acids. *Peptides* **2002**, *27*, 416−417.

(20) Andersen, N. H.; Liu, Z.; Prickett, K. S. Efforts toward Deriving the CD Spectrum of a 310 Helix in Aqueous Medium. *FEBS Lett.* **1996**, *399* (1−2), 47−52.

(21) Lau, S. Y.; Taneja, A. K.; Hodges, R. S. Synthesis of a Model Protein of Defined Secondary and Quaternary Structure. Effect of Chain Length on the Stabilization and Formation of Two-Stranded Alpha-Helical Coiled-Coils. *J. Biol. Chem.* **1984**, *259* (21), 13253−13261.

(22) Park, K.; Perczel, A.; Fasman, G. D. Differentiation between Transmembrane Helices and Peripheral Helices by the Deconvolution of Circular Dichroism Spectra of Membrane Proteins. *Protein Sci.* **1992**, *1* (8), 1032−1049.

(23) Jin, Y.; Mozsolits, H.; Hammer, J.; Zmuda, E.; Zhu, F.; Zhang, Y.; Aguilar, M. I.; Blazyk, J. Influence of Tryptophan on Lipid Binding of Linear Amphipathic Cationic Antimicrobial Peptides. *Biochemistry* **2003**, *42* (31), 9395−9405.

(24) Amos, S.-B. T. A.; Vermeer, L. S.; Ferguson, P. M.; Kozlowska, J.; Davy, M.; Bui, T. T.; Drake, A. F.; Lorenz, C. D.; Mason, A. J. Antimicrobial Peptide Potency Is Facilitated by Greater Conformational Flexibility When Binding to Gram-Negative Bacterial Inner Membranes. *Sci. Rep.* **2016**, *6* (1), 37639.

(25) Sani, M.-A.; Whitwell, T. C.; Separovic, F. Lipid Composition Regulates the Conformation and Insertion of the Antimicrobial Peptide Maculatin 1.1. *Biochim. Biophys. Acta, Biomembr.* **2012**, *1818* (2), 205−211.

(26) Shai, Y. Mode of Action of Membrane Active Antimicrobial Peptides. *Biopolymers* **2002**, *66* (4), 236−248.

(27) Brogden, K. A. Antimicrobial Peptides: Pore Formers or Metabolic Inhibitors in Bacteria? *Nat. Rev. Microbiol.* **2005**, *3* (3), 238−250.

(28) Jamasbi, E.; Mularski, A.; Separovic, F. Model Membrane and Cell Studies of Antimicrobial Activity of Melittin Analogues. *Curr. Top. Med. Chem.* **2016**, *16* (1), 40−45.

(29) McCoy, L. S.; Roberts, K. D.; Nation, R. L.; Thompson, P. E.; Velkov, T.; Li, J.; Tor, Y. Polymyxins and Analogs Bind to Ribosomal RNA and Interfere with Eukaryotic Translation in Vitro. *ChemBioChem* **2013**, *14* (16), 2083−2086.

(30) AL-Ani, I.; Zimmermann, S.; Reichling, J.; Wink, M. Pharmacological Synergism of Bee Venom and Melittin with Antibiotics and Plant Secondary Metabolites against Multi-Drug Resistant Microbial Pathogens. *Phytomedicine* **2015**, *22* (2), 245−255.

(31) Matsuzaki, K.; Sugishita, K.; Fujii, N.; Miyajima, K. Molecular Basis for Membrane Selectivity of an Antimicrobial Peptide, Magainin 2. *Biochemistry* **1995**, *34* (10), 3423−3429.

(32) Juretić, D.; Vukičević, D.; Petrov, D.; Novković, M.; Bojović, V.; Lučić, B.; Ilić, N.; Tossi, A. Knowledge-Based Computational Methods for Identifying or Designing Novel, Non-Homologous Antimicrobial Peptides. *Eur. Biophys. J.* **2011**, *40* (4), 371−385.

(33) Kamech, N.; Vukičević, D.; Ladram, A.; Piesse, C.; Vasseur, J.; Bojović, V.; Simunić, J.; Juretić, D. Improving the Selectivity of Antimicrobial Peptides from Anuran Skin. *J. Chem. Inf. Model.* **2012**, *52* (12), 3341−3351.

(34) Kuipers, B. J. H.; Gruppen, H. Prediction of Molar Extinction Coefficients of Proteins and Peptides Using UV Absorption of the Constituent Amino Acids at 214 Nm To Enable Quantitative Reverse

DOI: 10.1021/acs.jmedchem.7b01831
J. Med. Chem. 2018, 61, 2924−2936

Phase High-Performance Liquid Chromatography−Mass Spectrometry Analysis. *J. Agric. Food Chem.* **2007**, *55* (14), 5445−5451.
(35) Morgera, F.; Vaccari, L.; Antcheva, N.; Scaini, D.; Pacor, S.; Tossi, A. Primate Cathelicidin Orthologues Display Different Structures and Membrane Interactions. *Biochem. J.* **2009**, *417* (3), 727−735.
(36) Chen, Y.-H.; Yang, J. T.; Chau, K. H. Determination of the Helix and β Form of Proteins in Aqueous Solution by Circular Dichroism. *Biochemistry* **1974**, *13* (16), 3350−3359.
(37) The European Committee on Antimicrobial Susceptibility Testing. Breakpoint Tables for Interpretation of MICs and Zone Diameters. Version 7.1, 2017. http://www.eucast.org (accessed May 7, 2017).
(38) Louise Meyer, R.; Zhou, X.; Tang, L.; Arpanaei, A.; Kingshott, P.; Besenbacher, F. Immobilisation of Living Bacteria for AFM Imaging under Physiological Conditions. *Ultramicroscopy* **2010**, *110* (11), 1349−1357.
(39) Alves, C. S.; Melo, M. N.; Franquelim, H. G.; Ferre, R.; Planas, M.; Feliu, L.; Bardaji, E.; Kowalczyk, W.; Andreu, D.; Santos, N. C.; Fernandes, M. X.; Castanho, M. A. R. B. *Escherichia Coli* Cell Surface Perturbation and Disruption Induced by Antimicrobial Peptides BP100 and PepR. *J. Biol. Chem.* **2010**, *285* (36), 27536−27544.
(40) Singh, N. P.; McCoy, M. T.; Tice, R. R.; Schneider, E. L. A Simple Technique for Quantitation of Low Levels of DNA Damage in Individual Cells. *Exp. Cell Res.* **1988**, *175* (1), 184−191.
(41) Gajski, G.; Jelčić, Z.; Oreščanin, V.; Gerić, M.; Kollar, R.; Garaj-Vrhovac, V. Physico-Chemical Characterization and the in Vitro Genotoxicity of Medical Implants Metal Alloy (TiAlV and CoCrMo) and Polyethylene Particles in Human Lymphocytes. *Biochim. Biophys. Acta, Gen. Subj.* **2014**, *1840* (1), 565−576.
(42) Xu, D.; Zhang, Y. Ab Initio Protein Structure Assembly Using Continuous Structure Fragments and Optimized Knowledge-Based Force Field. *Proteins: Struct., Funct., Genet.* **2012**, *80* (7), 1715−1735.
(43) Pronk, S.; Pall, S.; Schulz, R.; Larsson, P.; Bjelkmar, P.; Apostolov, R.; Shirts, M. R.; Smith, J. C.; Kasson, P. M.; van der Spoel, D.; Hess, B.; Lindahl, E. GROMACS 4.5: A High-Throughput and Highly Parallel Open Source Molecular Simulation Toolkit. *Bioinformatics* **2013**, *29* (7), 845−854.
(44) Oostenbrink, C.; Villa, A.; Mark, A. E.; Van Gunsteren, W. F. A Biomolecular Force Field Based on the Free Enthalpy of Hydration and Solvation: The GROMOS Force-Field Parameter Sets 53A5 and 53A6. *J. Comput. Chem.* **2004**, *25* (13), 1656−1676.
(45) Poger, D.; Van Gunsteren, W. F.; Mark, A. E. A New Force Field for Simulating Phosphatidylcholine Bilayers. *J. Comput. Chem.* **2010**, *31* (6), 1117−1125.
(46) Berendsen, H. J. C.; Grigera, J. R.; Straatsma, T. P. The Missing Term in Effective Pair Potentials. *J. Phys. Chem.* **1987**, *91* (24), 6269−6271.
(47) Kandt, C.; Ash, W. L.; Peter Tieleman, D. Setting up and Running Molecular Dynamics Simulations of Membrane Proteins. *Methods* **2007**, *41* (4), 475−488.
(48) GROMACS Tutorials. http://www.bevanlab.biochem.vt.edu/Pages/Personal/justin/gmx-tutorials/ (accessed May 9, 2017).
(49) Parrinello, M.; Rahman, A. Polymorphic Transitions in Single Crystals: A New Molecular Dynamics Method. *J. Appl. Phys.* **1981**, *52* (12), 7182−7190.
(50) Berendsen, H. J. C.; Postma, J. P. M.; van Gunsteren, W. F.; DiNola, A.; Haak, J. R. Molecular Dynamics with Coupling to an External Bath. *J. Chem. Phys.* **1984**, *81* (8), 3684−3690.
(51) Hess, B.; Bekker, H.; Berendsen, H. J.; Fraaije, J. G.; et al. LINCS: A Linear Constraint Solver for Molecular Simulations. *J. Comput. Chem.* **1997**, *18* (12), 1463−1472.
(52) Essmann, U.; Perera, L.; Berkowitz, M. L.; Darden, T.; Lee, H.; Pedersen, L. G. A Smooth Particle Mesh Ewald Method. *J. Chem. Phys.* **1995**, *103* (19), 8577−8593.
(53) Kabsch, W.; Sander, C. Dictionary of Protein Secondary Structure: Pattern Recognition of Hydrogen-Bonded and Geometrical Features. *Biopolymers* **1983**, *22* (12), 2577−2637.
(54) Delano, W. The PyMOL Molecular Graphics System. http://www.pymol.org (accessed May 9, 2017).

DOI: 10.1021/acs.jmedchem.7b01831
J. Med. Chem. 2018, 61, 2924−2936